Estimation of surface-layer scaling parameters in the unstable boundary layer: implications for orographic flow speed-up

Article

Accepted Version

Argain, J. L., Teixeira, M. and Miranda, P. M. A. (2017) Estimation of surface-layer scaling parameters in the unstable boundary layer: implications for orographic flow speed-up. Boundary-Layer Meteorology, 165 (1). pp. 145-160. ISSN 0006-8314 doi: https://doi.org/10.1007/s10546-017-0260-3 Available at http://centaur.reading.ac.uk/70672/

Estimation of surface-layer scaling parameters in the unstable boundary-layer: implications for orographic flow speed-up

José Luís Argaín • Miguel A. C. Teixeira • Pedro M. A. Miranda

Received: DD Month YEAR/ Accepted: DD Month YEAR

Abstract A method is proposed for estimating the surface-layer depth (z_s) and the friction velocity (u_*) as a function of stability (here quantified by the Obukhov length, L) over the complete range of unstable flow regimes. This method extends the one developed previously by the authors for stable conditions in Argaín et al. (Boundary-Layer Meteorol, 2009, Vol.130, 15-28), but uses a qualitatively different approach. The method is specifically used to calculate the fractional speed-up (ΔS) in flow over a ridge, although it is suitable for more general boundary-layer applications. The behaviour of $z_s(L)$ and $u_*(L)$ as a function of L is indirectly assessed via calculation of $\Delta S(L)$ using the linear model of Hunt et al. (Q J R Meteorol Soc, 1988, Vol.29, 16-26) and its comparison with the field measurements reported in Coppin et al. (Boundary-Layer Meteorol, 1994, Vol.69, 173-199) and with numerical simulations carried out using a nonlinear numerical model, FLEX. The behaviour of ΔS estimated from the linear model is clearly improved when u_* is calculated using the method proposed here, confirming the importance of accounting for the dependences of $z_s(L)$ and $u_*(L)$ on L to better represent processes in the unstable boundary-layer.

José Luis Argaín
Departamento de Física, FCT, Universidade do Algarve, Faro 8005-139, Portugal.
jargain@ualg.pt

Miguel Ângelo Cortez Teixeira
Department of Meteorology, University of Reading, Earley Gate, PO Box 243, Reading RG6 6BB, UK
m.a.teixeira@reading.ac.uk

Pedro Manuel Alberto de Miranda
Instituto Dom Luiz, Faculdade de Ciências, Universidade de Lisboa, Lisbon 1749-016, Portugal
pmmiranda@fc.ul.pt

Keywords Convective boundary layer · Flow speed-up · Friction velocity · Surface-layer height · Unstable stratification

1 Introduction

Fractional speed-up (ΔS) of flow over hills or mountains is defined as the ratio of the speed perturbation at a given height to the upstream, unperturbed flow speed at the same height. This quantity is highly relevant both from meteorological and wind engineering perspectives, since it characterizes the modulation of the wind speed by orography. Hunt et al. (1988) (hereafter HLR) developed one of the first theoretical linear atmospheric boundary layer (ABL) models of flow over hills, which is one of the simplest and computationally cheapest tools available for estimating ΔS.

However, stratification affects ΔS and must be carefully accounted for in the evaluation of the scaling parameters that characterize the ABL. Among these, a key parameter is the friction velocity (u_*), and another one is the surface-layer depth (z_s), usually estimated as 5% to 10% of the ABL depth.

Weng (1997) (hereafter W97), after implementing a continuous wind profile in the HLR model, found that his predictions of ΔS disagreed significantly with the observations of Coppin et al. (1994) (hereafter C94). Argaín et al. (2009) (hereafter A09) showed that these discrepancies were due to the fact that the calculations in W97 were carried out assuming that u_* is constant, regardless of the different observed stability regimes. They proposed a method for estimating u_* in stably-stratified flows, which has led to an improved prediction of ΔS over 2D hills. C94 also compared their observations with predictions from the HLR model, and found considerable disagreement, both in stable and unstable conditions. Here we show that, as in stably-stratified flows, a decisive reason for such disagreements in unstable flow is the assumption of constant u_*.

In the present study, a new method is developed for estimating z_s and u_* as a function of stability (here quantified by the Obukhov length, L) over the complete unstable stratification range, i.e. from the free-convection to the neutral stability limits. Procedures are developed for estimating z_s in a neutral ABL, and for estimating this and several other scaling parameters, such as u_*, L and Deardorff's convective velocity scale, w_*, in the free-convection regime, which are preliminary steps for defining $z_s(L)$ and $u_*(L)$ for

all stabilities. Given that the physical processes taking place in the CBL and in an unstable surface layer are substantially different from those in a stable boundary ABL, the method used to represent them also differs substantially, requiring the use of additional theory.

The main motivation for developing this new method for estimating $z_s(L)$ and $u_*(L)$ is the calculation of $\Delta S(L)$ for unstable flow over hills, although it must be noted that the method can also be used for more general boundary layer applications. The calculation of $\Delta S(L)$ requires knowing $u_*(L)$ which, in the method proposed here, also requires estimating $z_s(L)$. The behaviour of $z_s(L)$ and $u_*(L)$ is thus indirectly assessed through the calculation of $\Delta S(L)$ using the HLR model. These predictions are compared with field measurements, reported in C94, and numerical simulations, carried out using a 2D microscale-mesoscale non-hydrostatic model, FLEX. These comparisons allow us to show how $z_s(L)$ and $u_*(L)$ are sometimes not estimated in a physically consistent way, a limitation that the present method aims to overcome.

Section 2 presents the method that accounts for unstable stratification in the ABL and its calibration. Section 3 describes the main results, namely comparisons between theory, numerical simulations and measurements, using the new unstable ABL formulation. Finally, Sect. 4 summarizes the main conclusions of this study.

2 Methodology

2.1 Unstable ABL model

Several studies show that the ABL, under moderately to strongly unstable stratification (usually known as CBL), can be represented by a simplified three-layer bulk model (e.g., Garratt 1992). This comprises a thin statically unstable surface layer of depth z_s, a well-mixed layer, of height z_i and depth $\Delta z_i = z_i - z_s$, and a transition layer of thickness Δz_{ci}, coinciding with a temperature inversion capping the mixed layer, which inhibits vertical mixing. In the mixed layer, quantities such as the mean potential temperature (θ) and wind velocity (U,V) are well-mixed, and therefore constant with height, i.e. $\theta(z) = const.$, $U(z) = const.$ and $V(z) = 0$. For our purposes, the strict fulfilment of these profile shapes in the mixed layer is not critical, since we are essentially interested in the surface layer, for which typically $z_s \approx 0.05 z_i$ to $0.1 z_i$ (Stull 1988). In the surface layer we

assume that the turbulent shear stresses have much more important effects on the mean flow than the Coriolis force. Hence, the Coriolis parameter (f) is set to zero, except where otherwise explicitly stated. Since the surface layer has characteristics which make it markedly different from the mixed layer, z_s can be defined as an important length scale of the ABL, essential for describing the impact of the orography on the wind profile. This follows McNaughton (2004), who established z_s as a new basis parameter for similarity models of the surface layer. In the method proposed here, z_s is essential for estimating the key velocity scale, u_*, and hence for calculating $\Delta S(L)$.

2.2 Surface-layer model

According to Monin-Obukhov similarity theory (MOST), in the surface layer the non-dimensional vertical gradients of $U(z)$ and $\theta(z)$ are universal functions of the parameter z/L, taking the forms

$$\Phi_m\left(\frac{z}{L}\right)=\frac{\kappa z}{u_*}\frac{\partial U}{\partial z}, \tag{1}$$

and

$$\Phi_h\left(\frac{z}{L}\right)=\frac{\kappa z}{Pr_t\,\theta_*}\frac{\partial \theta}{\partial z}, \tag{2}$$

where z is the height above the effective ground level, κ is the von Kármán constant, Pr_t is the turbulent Prandtl number and θ_* represents the surface-layer scaling temperature. u_* and θ_*, are defined using the vertical eddy kinematic fluxes of momentum and heat at the surface, i.e. $u_*^2 = \left(\overline{w'u'}\right)_0$ and $\theta_* = -\left(\overline{w'\theta'}\right)_0/u_*$. The length L is given by

$$L=-\frac{\theta_0 u_*^3/\kappa}{g\left(\overline{w'\theta'}\right)_0}=\frac{\theta_0 u_*^2}{g\kappa\theta_*}, \tag{3}$$

where θ_0 is the potential temperature at the surface and g is the gravitational acceleration. Wilson (2001) (hereafter W01), after analyzing several forms of the functions Φ_m and Φ_h, proposed the following general form for the unstable regime ($z/L < 0$),

112 $$\Phi = \left(1 + \gamma \left|\frac{z}{L}\right|^{\alpha_1}\right)^{-\alpha_2}, \qquad (4)$$

113 which is valid for both Φ_m and Φ_h. He noted that in order to obtain the correct physical
114 behaviour for the gradients $\partial U/\partial z$ and $\partial\theta/\partial z$ in the free-convection limit ($z/L \to -\infty$), it
115 is required that $\alpha_1\alpha_2$ = 1/3. For this combination of values (4) behaves in this limit
116 similarly to 'classical' free-convection expressions, with $\partial U/\partial z$ and $\partial\theta/\partial z$ varying
117 proportionally to $z^{-4/3}$. He further noted that, for this choice of parameters, (1) - (2) may
118 be integrated straightforwardly. Following W01 we will use κ = 0.4, Pr_t = 0.95, γ_h =
119 7.86, $\alpha_{1m} = \alpha_{1h}$ = 2/3, $\alpha_{2m} = \alpha_{2h}$ = 1/2 and γ_m = 3.59.
120 Subscripted indices *s*, *n* and *fc* hereafter denote values of flow parameters in the surface
121 layer, in the neutral regime ($|L| \to \infty$), and in the free-convection regime ($|L| \to 0$),
122 respectively.
123 The method developed here requires that z_{sfc}, u_{*fc}, L_{fc}, z_{sn}, u_{*n} and z_0, be known in
124 order to calculate $u_*(L)$ and $z_s(L)$. The primary input parameters are u_{*n}, z_{ifc} and the
125 aerodynamic roughness height, z_0, which must be provided initially.
126
127 2.3 Estimating parameters in the free-convection and neutral regimes
128 MOST shows good agreement with observations in regimes with sufficiently strong
129 winds (high values of u_*) or under relatively low surface heat flux, $(\overline{w'\theta'})_0$, where $|L|$ >
130 10^2 m. This theory is based on the assumption that, in the surface layer, z and L are the
131 only relevant turbulence length scales. While this assumption is valid for relatively small
132 values of $|z/L|$ (say $|z/L|$ < 1), for larger values, in particular in the free-convection
133 regime, MOST becomes incomplete. In the perfectly windless regime, purely dominated
134 by thermal effects, both the mean wind speed and u_* approach zero, and MOST produces
135 singularities and underestimates the surface fluxes. However, perfectly windless
136 conditions occur very rarely, and the theory can still be applied, if conjugated with CBL
137 theory, for low but non-zero winds, as will be shown below.
138 For the highly convective ABL, Deardorff (1970) suggested the following convective
139 velocity scale

$$w_* = \left[\frac{g}{\theta_0} \left(\overline{w'\theta'} \right)_0 z_{ifc} \right]^{1/3} . \quad (5)$$

The combination of MOST and Deardorff similarity theory, adopted here, provides a model that is consistent throughout the whole CBL (Kaimal et al. 1976) (hereafter K76), and for stabilities ranging from the neutral regime to the free-convection regime. This latter regime does not strictly correspond to $L = 0$, but rather to a minimum, suitably small value of $L = L_{fc}$, to be determined. In the free-convection regime we need to estimate z_{sfc}, u_{*fc} and L_{fc}. Given that u_{*fc} is defined in relation to w_* (as shown below), this latter quantity, defined by (5), must also be related to the known input parameters. This requires a total of four equations (see below).

Many observations have confirmed that the transition from the shear-driven turbulent regime of the surface layer to the buoyancy driven regime of the mixed layer usually occurs at a height of order $|L|$. Hence, in a highly-convective ABL (Garratt 1992),

$$z_{sfc} = c_{fc} |L_{fc}| , \quad (6)$$

where $c_{fc} = 2$. Equation 6 will be adopted hereafter in the free-convection regime.

Based on observations, Schumann (1988) (hereafter S88) assumed that $z_s/z_i = 0.1$. As will be seen later, this assumption is too restrictive over the whole stability interval, since, z_i is expected to increase and z_s to decrease as the stratification becomes more unstable. A more general definition of z_s is thus required. This is developed in Sect. 2.4.

Businger (1973) proposed the idea that u_* does not vanish at low wind speeds, introducing the concept of a 'minimum friction velocity', valid in the free-convection regime ($u_{*min} = u_{*fc}$). Combining (3) and (5) in this regime, we obtain

$$\frac{\kappa |L_{fc}|}{z_{ifc}} = \left(\frac{u_{*fc}}{w_*} \right)^3 . \quad (7)$$

Using (6), it can be easily shown from (7) that z_{sfc}/z_{ifc} decreases as u_{*fc}/w_* decreases, which is physically plausible.

Various authors, such as S88 and Sykes et al. (1993) (hereafter S93), have advocated the view that u_{*fc}/w_* is a function of z_{sfc}/z_0 or z_{ifc}/z_0 as well. Following the less general relations derived by S88 and S93, valid only for limited intervals of z_0, Zilitinkevich et

al. (2006) (hereafter Z06) suggested a more complete formulation for the relationship between u_{*fc}/w_* and z_{ifc}/z_0, which takes into account the combined effects of buoyancy and shear forces,

$$\frac{u_{*fc}}{w_*} = c_1 \left[\ln \frac{z_{ifc}/z_0}{\left(\ln z_{ifc}/z_0 - c_0\right)^3} + c_2 \right]^{-1} \qquad \text{for } z_{ifc}/z_0 \geq \sigma, \tag{8}$$

$$\frac{u_{*fc}}{w_*} = c_3 \left[\frac{z_0}{z_{ifc}} + c_4 \left(\frac{z_0}{z_{ifc}} \right)^{8/7} \right]^{1/6} \qquad \text{for } z_{ifc}/z_0 < \sigma, \tag{9}$$

where σ = 3.45 × 10^5, $u_{*fc}/w_*(\sigma)$ = 0.065, c_0 = 6.00, c_1 = 0.29, c_2 = –2.56, c_3 = 0.54 and c_4 = 0.3. Equations 8 and 9 agree very well with both LES and field data in the free-convection regime (Z06), and incorporate the best characteristics of the S88 and S93 models.

The height z_i characterizes the PBL in a fairly integrated manner, being closely related to fundamental quantities such as $\left(\overline{w'\theta'}\right)_0$. For this reason, as a first approach, we suggest estimating the surface-layer scaling parameters in the free-convection regime based on a known value of z_{ifc}. This allows obtaining u_{*fc}/w_* directly from (8) - (9), since z_0 is also assumed to be known.

Our final constraint is based on Venkatram (1978) who, by using a simple mixed-layer model for the CBL, derived the following relationship between w_* and z_{ifc},

$$w_* = c_5 z_{ifc}, \tag{10}$$

where c_5 = 1.12 × 10^{-3} s^{-1}. Equation 10 compares extremely well with observations (see Appendix 2). Using the available value of z_{ifc}, (10) allows us to determine w_* directly.

Equations 6 - 10 may thus be used to obtain the surface-layer parameters in the free-convection regime, as follows. Given z_{ifc} and z_0, (8) or (9) is used to obtain u_{*fc}/w_* and (10) is used to obtain w_*, which yields u_{*fc}. Given z_{ifc}, w_* and u_{*fc}, determined in the preceding step, (7) is used to obtain L_{fc}. Finally, L_{fc} is inserted into (6) to obtain z_{sfc}. This yields u_{*fc}, L_{fc} and z_{sfc}, as required. Several different procedures analogous to the one just described would be possible, depending on what input parameters are known initially.

193 According to MOST, in the neutral regime

194 $$U_n(z) = \frac{u_{*n}}{\kappa} \ln\left(\frac{z}{z_0}\right). \quad (11)$$

195 Since, from (6), z_s is expected to depend on L, in the neutral regime at least (where no
196 stability effects exist), it seems reasonable to assume z_s to be a fixed fraction of z_i (Stull
197 1988),

198 $$z_{sn} = c_{SL}\, z_{in}, \quad (12)$$

199 where that fraction is conventionally defined as 5% to 10% of z_i (Stull 1988). In our
200 model, we assume c_{SL} = 0.05 (following Stull 2011). Here, and unlike what previous
201 authors have done, (12) is adopted only for the strictly neutral regime. As will be seen
202 later (Sect. 3.2), (12) holds approximately for a weakly unstable ABL, but not for a
203 strongly unstable ABL. In order to obtain z_{sn} from (12), it is still necessary to estimate
204 z_{in}. This can be done using the expression of Rossby and Montgomery (1935),

205 $$z_{in} = \frac{c_{zin} u_{*n}}{|f|}, \quad (13)$$

206 where c_{zin} = 0.2 (Garratt 1992).

207

208 2.4 Estimating z_s and u_* for arbitrary $L < 0$

209 The preceding section described the methodologies for estimating all the parameters
210 required for defining u_* and z_s in the free-convection and neutral regimes. Next we
211 explain the approach used to estimate these two parameters for arbitrary $L < 0$.

212 Since $|L|$ is the height at which the buoyant production of turbulence kinetic energy (E)
213 begins to dominate over shear production, the greater $\left(\overline{w'\theta'}\right)_0$ is (i.e. the smaller $|L|$ is),
214 the bigger Δz_i and the smaller z_s become, because convectively-driven turbulence
215 increasingly dominates over shear-driven turbulence. So, there is a clear relationship
216 between z_s and $|L|$ (expressed by (6) in the strongly unstable regime). However, for
217 intermediate unstable regimes the dependence $z_s(L)$ is not known.

218 Based on the ABL model described in Sect. 2.1, we define z_s as the height where the
219 vertical derivative of $\theta(z)$ reaches a small prescribed fraction of its surface value. Using

this property, in the present model $z_s(L)$ is determined by (see details in Appendix 1) evaluating the root of,

$$\frac{z_s}{z_{0\theta}} = \frac{1}{\alpha_{\Psi 2}}\left(\frac{z_{0\theta}}{z_s}\right)^{-\alpha_{\Psi 1}}\left[\frac{1+\gamma_h\left(z_s/|L|\right)^{\alpha_1}}{1+\gamma_h\left(z_{0\theta}/|L|\right)^{\alpha_1}}\right]^{-\alpha_2}, \qquad (14)$$

for any value of L, assuming that $z_{0\theta}$, α_1, α_2, γ_h, $\alpha_{\Psi 1}$ and $\alpha_{\Psi 2}$ are provided. As (14) includes the influence on $z_s(L)$ of parameters in both extremes of the stability interval (see Appendix 1), it is expected to provide a good approximation over the whole stability range. As the roughness length for heat, $z_{0\theta}$, is not provided by C94, we use here z_0 instead. Calculations not presented here show that the $z_s(L)$ dependences obtained using $z_{0\theta}/z_s$ or z_0/z_s are quite similar (the relation between $z_{0\theta}$ and z_0 assumed for this comparison follows Zilitinkevich 1995). Although $z_{0\theta}$ and z_0 differ, the proposed method for estimating z_s is not very sensitive to the exact value of z_0 as long as this is small.

$u_*(L)$, on the other hand, is calculated from

$$u_*(z_s, L) = \kappa z_s\left[1+\gamma_m\left(\frac{z_s}{|L|}\right)^{\alpha_1}\right]^{\alpha_2}\left(\frac{\partial U}{\partial z}\right)_{z_s}, \qquad (15)$$

where, in accordance with the slab model adopted initially (see Sect. 2.1), it is expected that $\partial U/\partial z$ becomes small as $z \to z_s$. Here we assume that in (15) the shear $(\partial U/\partial z)_{z_s}$ is constant, and, for convenience, equal to its neutral value. For $|L| \to \infty$ and at $z = z_s$, (1) reduces to $(\partial U/\partial z)_{z_{sn}} = u_{*n}/(\kappa z_{sn})$, in accordance with (11), where z_{sn} may be obtained from (12). The validity of the assumption $(\partial U/\partial z)_{z_s} = const.$ is tested in Appendix 2.

All quantities on the right-hand side of (15) are now known, and hence $u_*(z_s, L)$ may be determined in general. Finally, the $U(z)$ profile for the general unstably stratified case, which will be used in the HLR model for calculating $\Delta S(L)$,

$$U(z) = \frac{u_*}{\kappa}\left\{\ln\left(\frac{z}{z_0}\right) - 3\ln\left[\frac{1+\sqrt{1+\gamma_m\left(z/|L|\right)^{2/3}}}{1+\sqrt{1+\gamma_m\left(z_0/|L|\right)^{2/3}}}\right]\right\}, \qquad (16)$$

is obtained by integration of (1), using the velocity gradient expressed by (4) (see W01).

In the above treatment, it was assumed that the synoptic situation does not vary too rapidly compared with the time scales of flow over the ridge. Hence, according to MOST, the effect of L in the surface layer is dominant. As this quasi-steadiness is supported by the C94 campaign, the C94 observations can safely be used for testing the method proposed here. For more unsteady flows, it is likely necessary to use a time-dependent model for the whole ABL, such as that described by Weng and Taylor (2003), for providing upstream profiles $U(z)$ and $\theta(z)$ at different values of L. However, this approach would require more input parameters not available in the C94 observations, and their estimation would further increase the empiricism of the proposed method.

Summarizing, in this section, assuming that z_0, z_{sfc}, L_{fc}, z_{sn} and u_{*n} are known, we propose (14) and (15) for determining $z_s(L)$ and $u_*(L)$, respectively. $u_*(L)$ is then used in the HLR model to calculate $\Delta S(L)$ for flow over orography.

3 Results and discussion

The method presented above will be assessed using the observations of C94. These measurements were conducted during the Spring of 1984 and Summer of 1985, over Cooper's Ridge, located to the north-west of Goulburn, in New South Wales, Australia. This is a somewhat isolated north-south oriented, quasi-two-dimensional ridge of uniform low z_0, located along a valley that forces the air to flow over the hill predominantly from the west side. The windward slope of the ridge (west side) can be well fitted using a simple bell-shaped profile $h(x) = h_0/\{1 + (x/a)^2\}$ (with h_0 = 115 m and a = 400 m). The lee side of the ridge falls away to about $0.5h_0$ before rising to another broader ridge.

3.1 Estimation of parameter values from the data

As mentioned in Sect. 2, for determining $z_s(L)$ and $u_*(L)$, the method developed here requires that z_0, z_{sfc}, u_{*fc}, L_{fc}, z_{sn} and u_{*n} be known. From the data collected by C94, we have u_{*n} = 0.35 m s^{-1}, z_0 = 0.05 m and $f \approx 9 \times 10^{-5}$ s^{-1}. Using (13) we thus obtain z_{in} = 778 m, and using this value in (12) yields z_{sn} = 39 m.

The methodology described in Sect. 2.3 for estimating the flow parameters in the free-convection regime (z_{sfc}, u_{*fc}, L_{fc} and w_*) is now applied. As z_{ifc} is not supplied by C94, we will use a typical value corresponding to the season and latitude of the region

where the observations were taken. Figures containing the necessary information from ERA-40 Reanalysis, provided by Von Engeln and Teixeira (2013), suggest z_{ifc} = 1550 m. Next, since $z_{ifc}/z_0 = 3 \times 10^4 < \sigma = 3.45 \times 10^5$, we must use (9) to calculate $u_{*fc}/w_* = 0.098$. Substituting u_{*fc}/w_* and z_{ifc} into (7), we obtain L_{fc} = –3.6 m, and from (6) we obtain z_{sfc} = 7.2 m. Next, substitution of z_{ifc} in (10) gives w_* = 1.74 m s^{-1}, which in turn can be used for calculating u_{*fc} from $u_{*fc}/w_* = 0.098$, yielding u_{*fc} = 0.17 m s^{-1}. Table 1 presents known and estimated parameters of the ABL in the free-convection regime, obtained by the present method and, for comparison, observations from runs 6A1 and 6A2 of the field experiment reported by K76, corresponding to a highly convective ABL. As can be seen, the method proposed here seems to predict realistic results.

Source	u_{*fc} (m s^{-1})	$\lvert L_{fc}\rvert$ (m)	z_{sfc} (m)	z_{ifc} (m)	z_{sfc}/z_{ifc}	w_* (m s^{-1})	u_{*fc}/w_*
Present method	0.17	3.6	7.2	1550	0.005	1.70	0.098
Run 6A1	0.24	5.7	10.4	2095	0.005	2.43	0.099
Run 6A2	0.23	6.4	12.8	2035	0.006	2.21	0.104

Table 1 Parameters of the ABL in the free-convection regime. Line 1: parameters used in the present method. Lines 2-3: similar parameters from runs 6A1 and 6A2 of the experiment described in Kaimal et al. (1976). The value of z_{sfc} for these runs was obtained from (6).

It is interesting that, contrary to what happens in the neutral regime, the ratio z_{sfc}/z_{ifc} = 0.005, estimated above, is significantly lower than the value assumed in (12). This value is of the same order of magnitude as those derived from the measurements of K76, taken in strongly convective conditions (see Table 1). As pointed out before, the smaller $|L|$ is, the more intense the turbulent mixing by large convective eddies in the mixed layer becomes, thereby reducing z_s. This corroborates, using real data, that the neutral approximation for z_{sn}/z_{in} cannot be considered realistic over the whole range of variation of L, particularly near the free-convection regime.

3.2 Behaviour of z_s as a function of L

For a better understanding of the surface-layer structure, it is useful to define a transition height, z_{tr}, at which the convective contribution to $U(z)$ is as important as that of the

neutral log law. Following Kader and Yaglom (1990), from the W01 formulation (4), we can define

$$z_{tr} = |L| \gamma_m^{-1/\alpha_1}. \quad (17)$$

It is expected that, in moderately to strongly unstable flow regimes $z_{tr} < z_s$, i.e. at the top of the surface layer $U(z)$ is no longer logarithmic.

Figure 1 presents the variation of z_s and z_{tr}, with $|L|$, normalized by z_{sn}. The solid line represents $z_s(L)$, computed using (14). In (14), the coefficients $\alpha_{\Psi 1}$ and $\alpha_{\Psi 2}$, given by (23), take the values 0.415 and 0.018, respectively. $z_{tr}(L)$ (dashed line) is computed using (17).

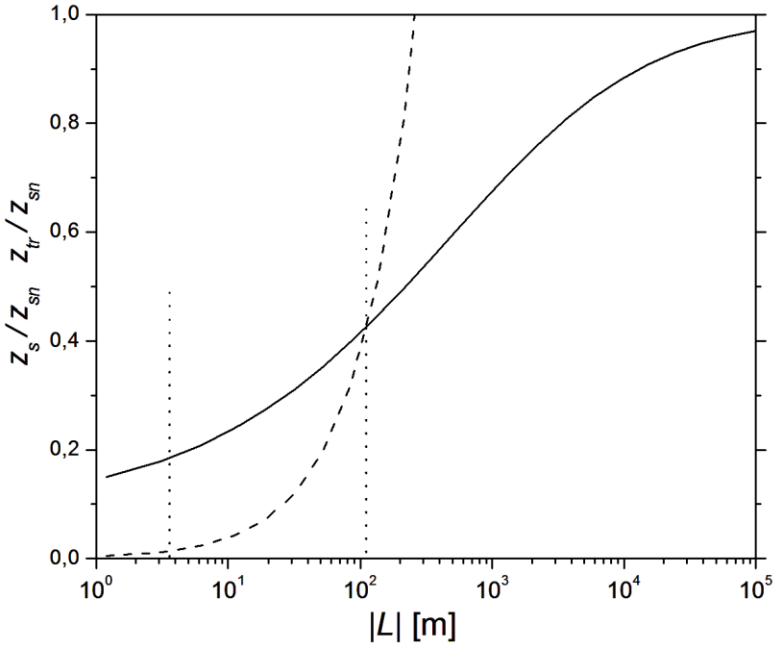

Fig 1 Surface-layer height, z_s, and transition height, z_{tr}, as a function of $|L|$, normalized by the surface-layer height for a neutral ABL, z_{sn}. Solid line: $z_s(L)$ obtained from (14), dashed line: $z_{tr}(L)$ obtained from (17). Vertical dotted lines: $|L_{fc}|$ = 3.6 m (left), and $|L_{tr}|$ = 120 m (right). $z_s(L)$ asymptotically approaches the constant values z_{sn} as $|L| \to \infty$ and $z_s(L)$ = 4.5 m as $|L| \to 0$. $z_s(L_{fc}) = z_{sfc}$ = 7.2 m (see Table 1).

The dotted vertical lines correspond to $|L_{fc}|$ = 3.6 m (left) as determined previously (see Table 1), and the value of $|L_{tr}|$ = 120 m (right) for which $z_s(L) = z_{tr}(L)$, i.e. for which the logarithmic and convective contributions to $U(z)$ are equally important. For $|L|$ > 400 m the logarithmic portion of $U(z)$ is overwhelmingly dominant compared to the

convective one, and therefore it can be considered that the ABL is in nearly neutral conditions. For $L = L_{fc}$ or lower, the opposite is true, as the flow is nearly in free-convection conditions. $z_s(L)$ physically behaves as expected, tending asymptotically to constant values at each extreme of the stability interval (4.5 m as $|L| \rightarrow 0$, and z_{sn} for $|L| \rightarrow \infty$). Figure 1 illustrates the way in which the surface layer becomes thinner with increasing unstable stratification, because of the progressively higher buoyant production of E in the mixed layer as $|L|$ decreases.

3.3 Behaviour of u_* as a function of L

Figure 2 presents u_* as a function of $|L|$, normalized by u_{*n}. The solid line corresponds to $u_*(L)$ computed from (15), and the dash-dotted line extends the constant neutral value, u_{*n} = 0.35 m s^{-1}, over the whole stability interval, for comparison. Figure 2 shows that $u_*(L)$ decreases with decreasing $|L|$ until it reaches its minimum value (u_{*min}) at $L = |L_{min}|$. According to (15), for $|L| < |L_{min}|$, $u_*(L)$ would increase monotonically with decreasing $|L|$, in such a way that $u_*(L) \rightarrow \infty$ for $|L| \rightarrow 0$. This behaviour occurs because, as $|L| \rightarrow 0$, the term between brackets on the right-hand side of (15) tends to infinity. This is a consequence of the physically unrealistic behaviour of MOST as $|L| \rightarrow 0$, producing singularities. For this reason, in Fig. 2 we have assumed that $u_*(L) = u_{*min}$, for $|L| \leq |L_{min}|$.

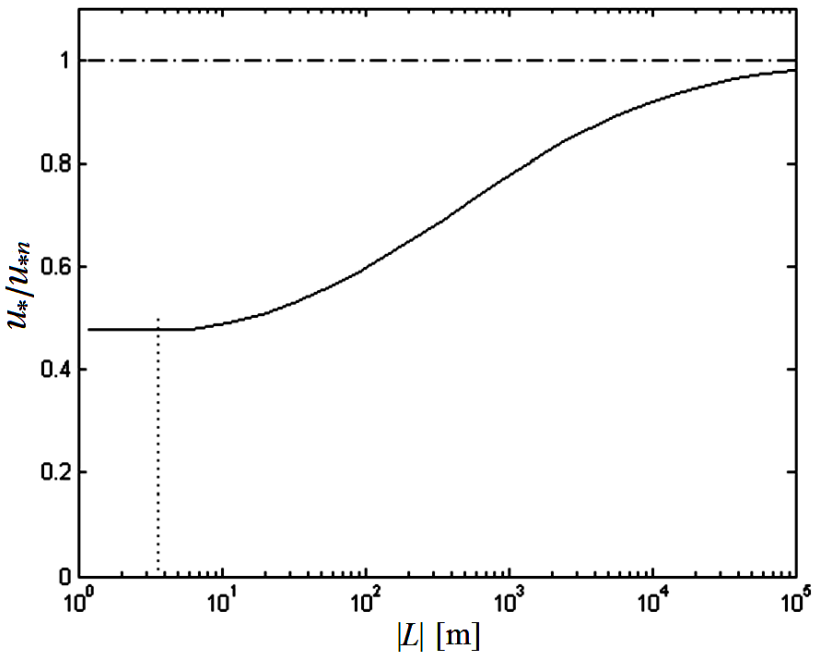

Fig 2 Friction velocity (u_*) as a function of $|L|$, obtained from (15) (solid line) and constant u_* independent of the stability and equal to its value in the neutral regime (u_{*n} = 0.35 m s^{-1}) (dash-dotted line). Both quantities are normalized by u_{*n}. The vertical dotted line indicates the value of L in the free-convection regime, $|L_{fc}|$ = 3.6 m (see Table 1).

As can be seen in Fig. 2, $u_*(L)$ shows the expected physical behaviour (cf. Fig. 3.7 of Garratt 1992), approaching asymptotically (by design) u_{*n} as $|L| \to \infty$, and decreasing monotonically with decreasing $|L|$. However, the approach to u_{*n} as $|L| \to \infty$ is very gradual and u_* only takes a value mid-way between the neutral and free-convection limits for an $|L|$ of several hundred metres. Furthermore, the minimum value reached by $u_*(L)$ is u_{*min} = 0.17 m s^{-1} for L_{min}= 3.4 m. Thus, $u_{*min} = u_{*fc}$ and $|L_{min}|$ almost coincides with $|L_{fc}|$= 3.6 m, determined previously (see Table 1). This result further confirms that the assumption of constant $(\partial U/\partial z)_{z_s}$ is realistic, and allows obtaining reliable estimates of u_* over the whole stability interval.

Although u_{*fc}, is thus a minimum value of u_*, it is generally not as low compared with u_{*n} as might be expected. The case under consideration here, where $u_{*fc}/u_{*n} \approx 0.5$, which is not particularly low (see Sect. 3.1, Table 1), is a good example. This result ultimately suggests that a purely-thermal regime is unlikely (it was not realized in the C94 measurements, in particular). For these reasons, under nearly free-convection

conditions both u_{*fc} and L_{fc} differ substantially from zero, as is confirmed by the observations of K76 (see Table 2), and further corroborated for a very unstable surface-layer case by Steeneveld et al. (2005). This is what allows MOST to be used here for describing a highly convective ABL.

3.4 Flow speed-up calculation

Since calculating $\Delta S(L)$ using the HLR model requires knowing $u_*(L)$, the main purpose of this section is to use the behaviour of $\Delta S(L)$ predicted by that model to indirectly assess the dependence on stability of $u_*(L)$ (and also of $z_s(L)$) established in the method proposed here, by comparison with values of ΔS measured over a wide range of L by C94, and simulated numerically using the FLEX model.

Suppose that at a hilly location $\Delta S(L)$ needs to be estimated, assuming that the only available parameters are z_0 and the mean wind speed, $U(z)$, measured at a suitably low height such that, according to MOST, (11) is approximately valid for any L. Equation 11 can then be used for estimating u_{*n}. Once z_0 and u_{*n} are known, the present method allows systematically obtaining $z_s(L)$, then $u_*(L)$ and finally $\Delta S(L)$, for the whole unstable stratification parameter range.

In the specific case under consideration here, first using as input parameters u_{*n} = 0.35 m s^{-1} and z_0 = 0.05 m (from C94), $u_*(L)$ is calculated using the proposed method. Next, this $u_*(L)$ is used in the HLR model applied to flow over Cooper's ridge to calculate $\Delta S(L)$. $\Delta S(L)$ is also calculated assuming that $u_* = const. = u_{*n}$, regardless of the observed L. This simpler choice, often used for estimating $\Delta S(L)$ in flow over orography (e.g. W97), is what the present approach aims to improve. Finally, the ΔS values are compared, for a range of L, between the HLR model, the C94 measurements, and the FLEX model.

For the sake of simplicity the HLR and FLEX models are not described in detail here. A brief description of the HLR model can be found in W97 or A09. FLEX is a microscale-mesoscale, nonlinear and non-hydrostatic model, which was developed and validated against experimental and field data by Argaín (2003) and A09. This model has been tested and used extensively, namely by Teixeira et al. (2012, 2013a, 2013b) for assessing analytical mountain wave drag predictions in 2D flows by comparison with numerical simulations.

All the numerical simulations presented here used a main grid of (160 × 364) points for a domain of (8000 × 2000) m size. The horizontal domain extent is $20a$ ($7a$ upstream of the ridge maximum and $13a$ downstream). From z = 40 m downward the level of grid refinement is gradually increased, and the lowest level is at a similar distance to the surface as the observations (≈ 0.15 m). At the surface a no-slip condition is used, and $(\overline{w'\theta'})_0$ and other turbulent quantities (turbulent kinetic energy, E, and dissipation ε of E), are specified, for each L, by assuming that viscous dissipation balances shear and buoyancy production. At the upper boundary, constant U and θ are prescribed, and L and the derivatives of E and ε are set to zero.

Observations, and both theoretical and numerical predictions of ΔS as a function of $|L|$ are shown in Fig. 3, at z = 8 m and z = 16 m. The HLR model is applied in two cases: a) $u_* = u_{*n}$, regardless of $|L|$ (dashed line), and b) the friction velocity is calculated for each $|L|$, using the method proposed here (15) (solid line).

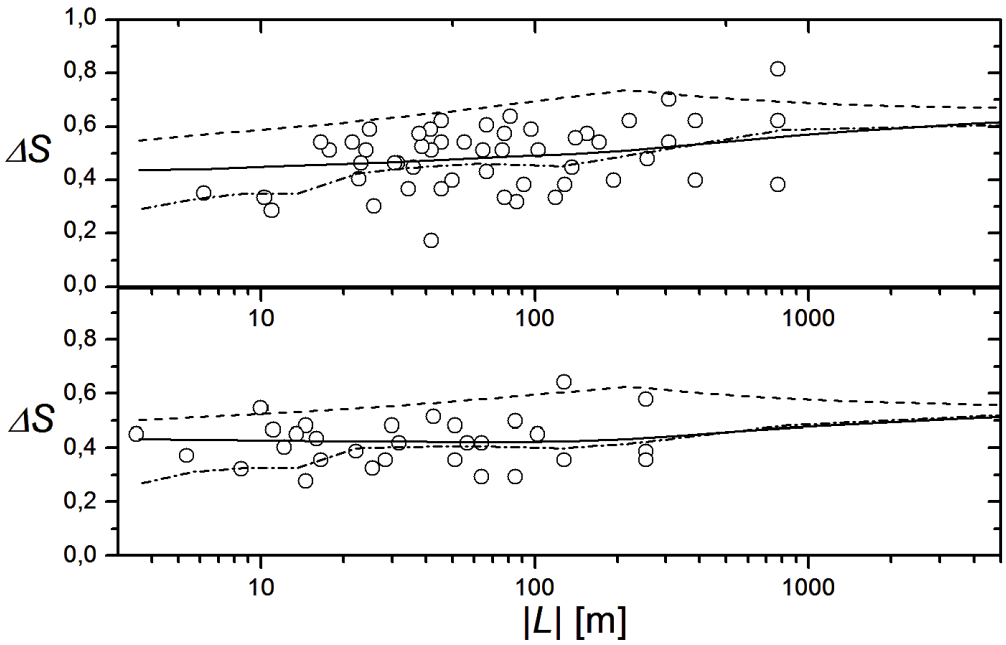

Fig 3 Variation of the fractional speed-up (ΔS) as a function of stability, above the hill crest, at the heights z= 8 m (top) and z = 16 m (bottom). Solid line: u_* computed using (15); dotted line: u_* kept constant, regardless of the stability, and equal to the neutral ABL value (u_{*n} = 0.35 m s^{-1}); dash-dotted line: FLEX model; symbols: observations from C94.

The significant differences between the ΔS curves, obtained using the two different definitions of u_*, reveals that ΔS is very sensitive to the dependence of u_* on $|L|$, as shown by A09 for the stable case. The results assuming $u_* = u_{*n}$ (dashed lines) overestimate the observations considerably. In both panels of Fig. 3, the improvement in the performance of the theoretical model, owing to the new method of calculating u_* (solid lines), is significant over the whole stability interval. In general, this new method produces results much closer to both the field measurements (despite the considerable scatter in the data) and the numerical simulation results. ΔS calculated from the theoretical model with u_* depending on L has a rather flat variation with $|L|$, especially at z = 16 m, and although decreasing more substantially with $|L|$ at z = 8 m, slightly overestimates both the measurements and the numerical simulations for the lowest values of $|L|$.

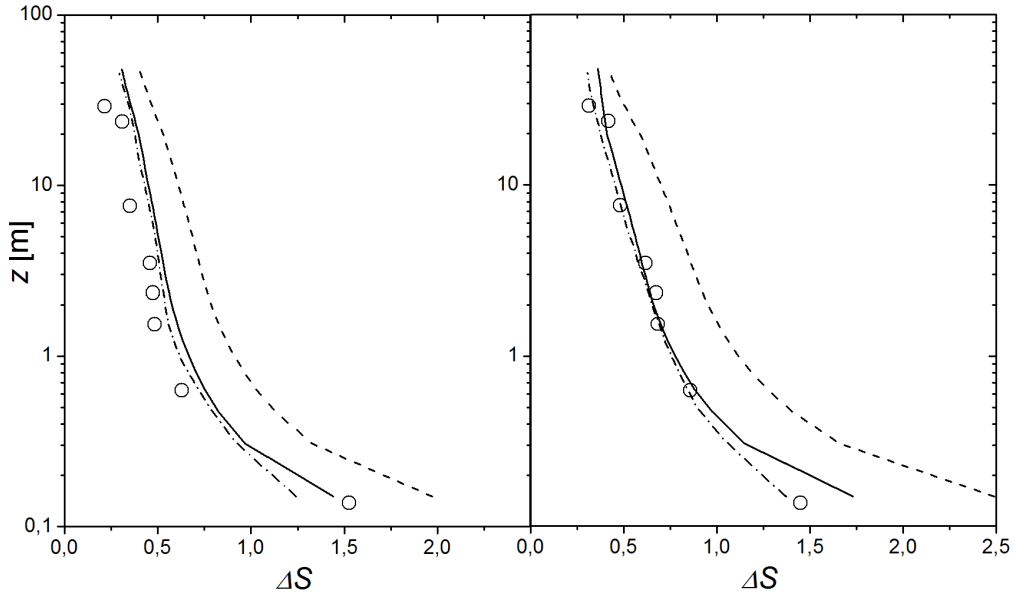

Fig 4 Profiles of the fractional speed-up ratio (ΔS) above the hill crest, for $|L|$ = 33 m (left) and $|L|$= 222 m (right). Solid line: u_* computed using (15); dashed line: u_* kept constant at u_{*n} = 0.35 m s^{-1}; dash-dotted line: FLEX model; symbols: observations from C94.

Profiles of observations (C94), and both theoretical and numerical predictions of ΔS directly above the hill crest, for $|L|$ = 33 m (left panel) and $|L|$ = 222 m (right panel) are shown in Fig. 4. $|L|$ = 33 m and $|L|$ = 222 m correspond to strong and moderately weak

unstable stratification, respectively. In both cases, the proposed method compares better both with the numerical model and with the field data, although it slightly overestimates the observations in the more unstable case. Nevertheless, a general decrease of ΔS as one shifts from the higher to the lower $|L|$ value is qualitatively reproduced. Given the precision of the measurements and flow assumptions, not too much importance should be attached to this overestimate, which also occurs in the numerical simulations (consistently, a similar discrepancy can be detected for the theoretical model on the far left of Fig. 3 at z = 8 m).

ΔS is much more severely overestimated, in both cases, by the profiles with a prescribed constant $u_* = u_{*n}$, due essentially to the significant fractional deviation between u_{*n} and the more accurate value of u_* determined from (15). This fractional deviation amounts to ~45% for $|L|$ = 33 m and to ~ 35% for $|L|$ = 222 m (see Fig. 2), but this does not translate into proportional deviations for ΔS, as the value of ΔS, where u_* is calculated from (15), actually becomes closer to that where $u_* = u_{*n}$ as $|L|$ decreases (see Fig. 3). The fact that there is such a large difference in the results using $u_*(L)$ and $u_* = u_{*n}$ for the weakly unstable case might seem suspect, but Fig. 2 explains it, since for $|L|$ = 222 m, $u_*(L)$ still differs very substantially from u_{*n}.

It should be pointed out that at the lowest measurement level, ΔS should depend very weakly on L, because near enough to the ground the flow is always approximately neutral. The overestimate of the measured ΔS at that level by the theoretical model for $|L|$ = 222 m can probably be attributed to an inherent bias of the HLR solution, noted by W97 and A09.

4 Summary and conclusions

In this paper, we propose a new method for estimating two scaling parameters of the ABL: the surface-layer height z_s and the friction velocity u_*, as a function of stability (quantified by the Obukhov length scale L), for an unstable ABL. These two parameters are important for characterizing the unstable ABL, in particular its coupling with the overlying convective mixed layer. Moreover, a correct estimation of u_*, whose dependence on L is often not accounted for in a physically consistent way, is crucial for

producing accurate predictions of the speed-up (ΔS) in flow over hills, which is relevant for a number of engineering applications.

Using a physical approach that is developed specifically for unstable conditions, via a combination of MOST and convective mixed-layer scaling, our model takes into account the fact that z_s decreases as the unstable stratification becomes stronger, due to erosion of the surface-layer eddies by more energetic buoyancy-dominated eddies from the convective mixed layer. The model also takes into account the fact that u_* decreases as the ABL becomes more unstable, attaining a minimum value, but does not, in general, approach zero in the free-convection limit, unless the wind vanishes completely (in which case the concept of ΔS loses its meaning). The variation of u_* affects the turbulent fluxes of various properties, and consequently the mean profiles of those properties, including the wind speed $U(z)$, which determines the behaviour of ΔS.

Procedures to obtain boundary-layer parameters in the neutral and free-convection regimes, and for bridging across these regimes, to cover the complete unstable ABL parameter range, were developed and tested using available field data. The performance of the model was then evaluated more comprehensively, by comparing predictions of ΔS in unstable conditions, using the linear model of HLR incorporating the new friction velocity formulation, against measurements from C94, and numerical simulations of the FLEX mesoscale-microscale model. Agreement was found to be substantially improved relative to results where u_* is held constant. This emphasizes the importance of accounting for the full dynamics of the unstable ABL, including the variation of u_* and z_s with stability, for correctly estimating ΔS. The proposed method, whose possible applications are not limited to improving the calculation of ΔS, should be seen as a preliminary step in the development of better tools for the parametrization of unstable ABLs. Further validation of this method by comparison with observations remains necessary.

Acknowledgements The authors thank two anonymous referees and the co-editors for insightful comments, which substantially improved this article. M.A.C.T. acknowledges the financial support of the European Commission, under Marie Curie Career Integration Grant GLIMFLO, contract PCIG13-GA-2013-618016. P.M.A.M. acknowledges the financial support of FCT, under Grant RECI/GEO-MET/0380/2012.

Appendix 1. Accuracy of the $(\partial\theta/\partial z)_{z_s} = const.$ approximation

In the present model, the form of $z_s(L)$ is established using the temperature gradient $\partial\theta/\partial z$, which can be obtained from (2) and (4), yielding

$$\frac{\partial\theta}{\partial z} = \theta_*' \left[1 + \gamma_h \left(\frac{z}{|L|} \right)^{\alpha_1} \right]^{-\alpha_2} z^{-1}, \tag{18}$$

where $\theta_*' = Pr_t \theta_* / \kappa$. According to (18), $\partial\theta/\partial z \to 0$ as $z \to \infty$. This is consistent with the assumption that $\theta = const.$ in the mixed layer, so, at $z = z_s$ the derivative $(\partial\theta/\partial z)_{z_s}$ should be suitably small, and this smallness is exploited to obtain z_s. Note that a similar condition could be based on the mean velocity gradient (1), but we think that $\theta = const.$ is more reliable in the mixed layer, since $U(z)$ profiles may exhibit non-negligible shear above the surface layer, due to variation of the pressure perturbation induced by the orography with height or the Coriolis force. Taking this into account, the ratio

$$\Psi(z_s, L) = \frac{(\partial\theta/\partial z)_{z_s}}{(\partial\theta/\partial z)_{z_{0\theta}}} = \left[\frac{1 + \gamma_h (z_s/|L|)^{\alpha_1}}{1 + \gamma_h (z_{0\theta}/|L|)^{\alpha_1}} \right]^{-\alpha_2} \frac{z_{0\theta}}{z_s}, \tag{19}$$

implicitly determines $z_s(L)$, if the form of the function $\Psi(z_s, L)$ is known. In (19) $(\partial\theta/\partial z)_{z_s}$ and $(\partial\theta/\partial z)_{z_{0\theta}}$ are obtained by evaluating (18) at z_s and the temperature roughness height, $z_{0\theta}$, respectively. As defined by (19), $\Psi(z_s, L)$ varies monotonically from 1 to zero as $z_{0\theta}/z_s$ decreases. Moreover, $\Psi(z_s, L)$ depends only weakly on L: by substituting L_{fc}, z_{sfc}, z_{sn} and $L_n = \infty$ (see Sect. 3.1, Table 1) into (19) we may calculate the ratio $\Gamma = \Psi(z_{sn}, L \to -\infty) / \Psi(z_{sfc}, L_{fc}) \approx 0.6$, which is of order 1.

The limits of $\Psi(z_s, L)$ at the theoretical extremes of the stability interval are, respectively,

$$\Psi_{sfc} = \Psi(z_{sfc}, L \to 0) = \lim_{|L|\to 0} \Psi(L) = \left(\frac{z_{0\theta}}{z_{sfc}} \right)^{\alpha_1\alpha_2+1}, \tag{20}$$

$$\Psi_{sn} = \Psi(z_{sn}, L \to \infty) = \lim_{|L|\to\infty} \Psi(L) = \frac{z_{0\theta}}{z_{sn}}. \tag{21}$$

For both strongly and weakly unstable flows, (20) - (21) suggest that $\psi(z_s, L) \propto (z_{0\theta}/z_s)^{\alpha}$, where α is a dimensionless constant. Taking this result into account, we

hypothesize that this form holds for the whole stability interval, yielding the following approximate definition for $\psi(z_s, L)$,

$$\Psi(z_s, L) = \alpha_{\Psi 2}\left(\frac{z_{0\theta}}{z_s}\right)^{\alpha_{\Psi 1}}, \tag{22}$$

where $\alpha_{\Psi 1}$ and $\alpha_{\Psi 2}$ are dimensionless constants. These two constants can be determined by taking the limits of (22) in the free-convection and neutral regimes, and comparing the corresponding expressions with (20) and (21), respectively. This produces a set of two equations, which may be solved for $\alpha_{\Psi 1}$ and $\alpha_{\Psi 2}$, yielding

$$\alpha_{\Psi 1} = \ln\left[\frac{\Psi(z_{sn}, L\to\infty)}{\Psi(z_{sfc}, L_{fc})}\right] \Big/ \ln\left(\frac{z_{sfc}}{z_{sn}}\right) \qquad \alpha_{\Psi 2} = \Psi(z_{sfc}, L_{fc})\left(\frac{z_{0\theta}}{z_{sfc}}\right)^{-\alpha_{\Psi 1}} \tag{23}$$

By combining (19) and (22), (14) is obtained.

Appendix 2. Accuracy of the $(\partial U/\partial z)_{z_s} = const.$ approximation

Here we show that the approximation $(\partial U/\partial z)_{z_s} = const.$, used in Sect. 2.4 for evaluating u_*, is supported by measurements. Let us consider the following ratio, by using MOST,

$$\beta_{MOST} = \frac{(\partial U/\partial z)_{z_{sn}}}{(\partial U/\partial z)_{z_{sfc}}} = \underbrace{\left(\frac{c_{fc}\beta_1 |f|}{c_{SL}c_{zin}}\right)}_{\alpha_5}\frac{|L_{fc}|}{u_{*fc}}, \tag{24}$$

where $\beta_1 = \left(1 + \gamma_m c_{fc}^{\alpha_1}\right)^{\alpha_2}$. Equation 24 is obtained by combining (1), (4), (6), (12) and (13). Using parameters from C94 (see Sect. 3.1) we obtain α_5 = 0.0466 s^{-1}. For the values of L_{fc} and u_{*fc} shown in Table 1, this yields β_{MOST} = 0.99. The remarkable closeness of this value to 1 is fortuitous, although it obviously depends on the values adopted for c_{zin}, c_{fc} and c_{SL}. For checking further the approximation $\beta_{MOST} \approx 1$ we use the K76 observations (keeping the same α_5), which were carried out in a daytime well-mixed CBL, with evidence of significant heat and momentum entrainment through the capping inversion.

Run	u_{*fc} (m s^{-1})	$\lvert L_{fc}\rvert$ (m)	z_{ifc} (m)	w_* (m s^{-1})	w_*/z_{ifc} (s^{-1})	β_{MOST}
6A1	0.24	5.7	2095	2.43	1.16×10^{-3}	1.1

6A2	0.23	6.4	2035	2.21	1.09×10^{-3}	1.3

Table 2 CBL parameters measured by Kaimal et al. (1976). Columns 6 and 7 show, respectively, w_*/z_{ifc}, and β_{MOST}, calculated from the data (the second quantity by using (24)).

Table 2 shows CBL parameters obtained by K76, corresponding to the runs with the smallest values of $|L|$, typical of nearly free-convection regimes. As can be seen, the values of β_{MOST} are close to 1, corroborating the hypothesis $\beta_{MOST} \approx 1$. Moreover, column 6 supports (10), proposed by Venkatram (1978), since $c_5 = w_*/z_{ifc}$ varies within a narrow range. Venkatram (1978) estimated $c_5 = 1.12 \times 10^{-3}$ s^{-1}, which is quite close to both values shown in Table 2. Therefore, the assumption that c_5 is a constant is plausible.

If the assumption $\beta_{MOST} = 1$ is accepted, (24) defines a relationship between α_5, $|L_{fc}|$ and u_{*fc}. If parameters c_{fc} and c_{zin} are assumed to be non-adjustable, this is equivalent to a relation between $|L_{fc}|$, u_{*fc} and c_{SL}. Equation 13 is only applicable if $|L| \to \infty$ (a rarely observed situation), so the parameter c_{zin} may have a considerable uncertainty. Zilitinkevich et al. (2012) and Garratt (1992) discuss this topic at length. It would be interesting to explore the constraint defined by (24) further to develop relations other than (13) for estimating z_{in}, but that is beyond the scope of the present paper.

We also carried out a similar analysis using the classical free-convection formulation of Prandtl (1932) for the mean velocity gradient,

$$\left(\frac{\partial U}{\partial z}\right)_{z_{sfc}} = \frac{c_u u_{*fc} (\kappa |L_{fc}|)^{1/3}}{z_{sfc}^{4/3}} = \frac{c_u \kappa^{1/3}}{c_{fc}^{4/3}} \frac{u_{*fc}}{|L_{fc}|}, \qquad (25)$$

where $c_u = 1.7$. In this case we would obtain a ratio $(\partial U/\partial z)_{z_{sfc}}/(\partial U/\partial z)_{z_{sn}}$ with a similar parameter dependence as (24) and $\alpha_5 = 0.0453$ s^{-1}. The proximity between the values of α_5 obtained using both formulations for $(\partial U/\partial z)_{z_{sfc}}$ confirms that the MOST formulation adopted here is physically consistent, hence it may be used to describe the free-convection regime.

References

Argaín JL (2003) Modelação de Escoamentos Atmosféricos: Efeitos Orográficos e de Camada Limite (in Portuguese). Ph.D. Thesis, Universidade do Algarve, 275 pp

572 Argaín JL, Miranda PMA, Teixeira MAC (2009) Estimation of the friction velocity in stably stratified
573 boundary-layer flows over hills. Boundary-Layer Meteorol 130: 15-28
574 Businger JA (1973) A Note on Free Convection. Boundary-Layer Meteorol 4: 323–326
575 Coppin PA, Bradley EF, Finnigan JJ (1994) Measurements of flow over an elongated ridge and its thermal
576 stability dependence: The mean field. Boundary-Layer Meteorol 69: 173-199
577 Deardorff JW (1970) Convective velocity and temperature-scales for the unstable planetary boundary layer.
578 J Atmos Sci 27: 1211–1213
579 Garratt JR (1992) The Atmospheric Boundary Layer, Cambridge University Press, 316 pp
580 Hunt JCR, Leibovich SL, Richards KJ (1988) Turbulent Shear Flows Over Low Hills. Q J R Meteorol Soc
581 29: 16-26
582 Kader BA, Yaglom AM (1990), Mean Fields and Fluctuation Moments in Unstably Stratified Turbulent
583 Boundary Layers, J Fluid Mech 212: 637–662
584 Kaimal JC, Wyngaard JC, Haugen DA, Cote OR, Izumi Y, Caughey SJ, Readings CJ (1976) Turbulence
585 Structure in the Convective Boundary Layer. J Atmos Sci 33: 2152-2169
586 McNaughton KG (2004) Turbulence Structure of the Unstable Atmospheric Surface Layer and Transition
587 to the Outer Layer. Boundary-Layer Meteorol 112: 199-221
588 Prandtl L (1932) Meteorologische Anvendungen der Str¨omungslehre. Beitr Phys Fr Atmos 19: 188-202
589 Rossby CG, Montgomery RB (1935) The layers of frictional influence in wind and ocean currents. Pap
590 Phys Oceanogr Meteorol 3: 101 pp
591 Schumann U (1988) Minimum Friction Velocity and Heat Transfer in the Rough Surface Layer of a
592 Convective Boundary Layer. Boundary-Layer Meteorol 44: 311–326
593 Steeneveld GJ, Holtslag AAM, DeBruin HAR (2005) Fluxes and gradients in the convective surface layer
594 and the possible role of boundary-layer depth and entrainment flux, Boundary-Layer Meteorol 116:
595 237-252
596 Stull, RB (1988) An Introduction to Boundary-Layer Meteorology, Kluwer Academic Publishers,
597 Dordrecht,, 670 pp
598 Stull, RB (2011) Meteorology for Scientists and Engineers, 3rd edition, University of British Columbia,
599 Vancouver British Columbia, 938 pp
600 Sykes RI, Henn DS, Lewellen WS (1993) Surface-layer description under free-convection conditions. Q J
601 R Meteorol Soc 119: 409–421
602 Teixeira MAC, Argaín JL, Miranda PMA (2012) The importance of friction in mountain wave drag
603 amplification by Scorer parameter resonance. Q J R Meteorol Soc 138: 1325-1337
604 Teixeira MAC, Argaín JL, Miranda PMA (2013a) Drag produced by trapped lee waves and propagating
605 mountain waves in a two-layer atmosphere. Q J R Meteorol Soc 139: 964-981
606 Teixeira MAC, Argaín JL, Miranda PMA (2013b) Orographic drag associated with lee waves trapped at an
607 inversion. J Atmos Sci 70: 2930–2947

608 Venkatram A (1978) Estimating the convective velocity scale for diffusion applications. Boundary-Layer
609 Meteorol 15: 447-452
610 Von Engeln A and Teixeira J (2013) A planetary boundary-layer height climatology derived from ECMWF
611 re-analysis data. J. Clim 26: 6575–6590
612 Weng W (1997) Stably stratified boundary-layer flow over low hills: A comparison of model results and
613 field data. Boundary-Layer Meteorol 85: 223-241
614 Weng W, Taylor PA (2003) On modelling the one-dimensional atmospheric boundary layer. Boundary-
615 Layer Meteorol., 107:371-400
616 Wilson DK (2001) An Alternative Function for the Wind and Temperature Gradients in Unstable Surface
617 Layers. Boundary-Layer Meteorol 99: 151–158
618 Zilitinkevich SS (1995) Non-local turbulent transport: Pollution dispersion aspects of coherent structure of
619 convective flows. Air Pollution Theory and Simulation. Power H, Moussiopoulos N, Brebbia CA, Eds.,
620 Vol. I, Air Pollution III, Computational Mechanics Publications, 53–60.
621 Zilitinkevich SS, Hunt JCR, Grachev AA, Esau IN, Lalas DP, Akylas E, Tombrou M, Fairall CW,
622 Fernando HJS, Baklanov AA, Joffre SM (2006) The influence of large convective eddies on the
623 surface-layer turbulence. Q J R Meteorol Soc 132: 1423-1456
624 Zilitinkevich SS, Tyuryakov SA, Troitskaya YI, Mareev EA (2012) Theoretical Models of the Height of
625 the Atmospheric Boundary Layer and Turbulent Entrainment at Its Upper Boundary. Izvestiya,
626 Atmospheric and Oceanic Physics 48(1): 133-142